LCLS-TN-01-12
December, 2001

CSR Wake for a Short Magnet in Ultrarelativistic Limit*

G. Stupakov and P. Emma
Stanford Linear Accelerator Center, Stanford University, Stanford, CA 94309

Abstract

Using results for the CSR wake in a short magnet (E. L. Saldin et. al, NIM **A398**, 373(1997)) we obtain expressions for the wake in the limit of very large values of the relativistic factor γ, $\gamma \to \infty$, for both the entrance and exit of the magnet. The analytical results are illustrated with numerical computation of the wakes, energy loss and energy spread for magnets of different lengths.

*Work supported by Department of Energy contract DE–AC03–76SF00515.

1 Introduction

When an electron moves in a bending magnet it emits synchrotron radiation and generates a wakefield that effects other electrons in the beam. This wake is usually called a Coherent Synchrotron Radiation (CSR) wake and for a steady state case it has been computed in Refs. [1, 2].

In practice, bending magnets are often not long enough to assume that the wake is in the steady state. In the case when the formation length for the radiation is comparable or larger than the magnet length the transient effects associated with the entrance to and exit from the magnet should be taken into account. The analysis of such wake for large, but finite, values of the relativistic factor γ has been carried out in Ref. [3]. The results of this paper can be used in computation for moderate values of $\gamma \sim 10 - 10^2$, however, for very large γ, calculations involve extremely small spatial scale $\sim R/\gamma^3$, where R is the bending radius. In many cases, when $\gamma \sim 10^3$, such scale cannot be resolved numerically and the algorithm fails. For such large values of γ a good approximation for the wake would be the limit $\gamma \to \infty$. One such formula is given in Ref. [3], but only for the wake at the entrance to the magnet.

In this paper, in Section 2, using the results of Ref. [3], we find the wake in the limit $\gamma \to \infty$ for all possible locations of the particle relative to the magnet. The obtained equations have been programmed in a computer code, and illustrative examples of the computed wake are presented in Section 3.

2 Calculation of the Wake

Following Ref. [3] we will consider four different cases of location of the observation point P and the position of the particle at the retarded time P' when the radiation was emitted. These are the cases A, B, C, and D shown in Fig. 3 of the cited paper. In case A, P is located inside the magnet and P' is in front of the magnet at the straight part of the orbit. In case B both points are inside the magnet, and in case C they both are outside with P beyond, and P' before the magnet. In case D, P is beyond and P' is inside the magnet.

In what follows we will use the notation of Ref. [3].

2.1 Case A

The wake in this case is given by Eq. (30) of Ref. [3]. The observation point is located at angle ϕ measured from the entrance to the magnet and the particle is located at distance $s - s'$ from this point upstream. The retarded position of the particle is at the distance y from the magnet entrance. We will use dimensionless y ($y/R \to y$), keep only the first term in the equation, assume $y \gg \phi$, and neglect small terms

$$w = -\frac{4\gamma^4}{R^2}\gamma^2 y^2 \frac{\gamma^2 y^2 + \gamma^4 y \phi^3}{(\gamma^2 y^2 + \gamma^4 \phi^4/4)^3} = -\frac{4}{R^2}\gamma^2 y^3 \frac{y + \gamma^2 \phi^3}{(y^2 + \gamma^2 \phi^4/4)^3}\,. \qquad (1)$$

The minus sign of the wake corresponds to the positive longitudinal electric field and means that a particle gains energy. From this equation we see that the wake, as a function of y is localized at $y \sim \gamma\phi^2$, so we can further neglect the first term in the numerator which is small compared with the second one. This yields

$$w \approx -\frac{4}{R^2}\frac{\gamma^4 y^3 \phi^3}{(y^2 + \gamma^2 \phi^4/4)^3}\,. \qquad (2)$$

The maximum of w is reached at $y = \gamma\phi^2/2$, so we will introduce a new variable $\xi = y/\gamma$

$$w = -\frac{4}{R^2}\frac{\gamma \xi^3 \phi^3}{(\xi^2 + \phi^4/4)^3}\,. \qquad (3)$$

The equation that relates ξ to $s - s'$ is Eq. (31) of Ref. [3] which we rewrite as

$$\frac{s - s'}{R} = \frac{1}{2\gamma}\xi + \frac{\phi^3}{6}\left(1 - \frac{3}{4}\frac{\phi}{\gamma\xi}\right)\,, \qquad (4)$$

where we kept terms up to order of γ^{-1} in the Taylor expansion. As we see, terms with ξ have a small factor γ^{-1} in front, which means that large variation of ξ will result in small changes of $s - s'$. Hence, this wake is localized in the vicinity $(s - s')/R \approx \phi^3/6$, and in the limit $\gamma \to \infty$ can be approximated by a delta-function

$$w \approx A\delta\left(\frac{s - s'}{R} - \frac{\phi^3}{6}\right)\,. \qquad (5)$$

To find the coefficient A, we need to integrate w over s using the relation $ds/R = (d\xi/2\gamma)(1 + \phi^4/4\xi^2)$ that follows from Eq. (4)

$$\int w ds = -\frac{2\phi^3}{R}\int_0^\infty \frac{\xi^3(1 + \phi^4/4\xi^2)}{(\xi^2 + \phi^4/4)^3} d\xi = -\frac{4}{R\phi}\,. \qquad (6)$$

It follows from Eq. (6)

$$w = -\frac{4}{R^2\phi}\delta\left(\frac{s-s'}{R} - \frac{\phi^3}{6}\right) . \tag{7}$$

If we want to calculate the wake $W(s)$ for a bunch with a longitudinal distribution function $\lambda(s)$ ($\int \lambda(s)ds = 1$), we have

$$W(s) = \int w(s-s')\lambda(s')ds' = -\frac{4}{R\phi}\lambda\left(s - \frac{R\phi^3}{6}\right) . \tag{8}$$

Note that this wake has a large formation length proportional to γ: $l_{\rm form} \sim yR \sim \gamma R\phi^2 \sim \gamma R(\sigma_z/R)^{2/3}$. If the vacuum chamber leading to the magnet has metal elements within this length, the resulting CSR wake can be modified by the interaction with the metal.

2.2 Case B

In this case the wake coincides with the steady state wake found in Refs. [1, 2]

$$w(s-s') = -\frac{2}{(3R^2)^{1/3}}\frac{\partial}{\partial s'}\frac{1}{(s-s')^{1/3}} . \tag{9}$$

This expression is valid for $s - s' < R\phi^3/24$, where ϕ is the angle measured from the beginning of the magnet to the observation point. Points with $s - s' > R\phi^3/24$ correspond to Case A, with the wake given by Eq. (7).

For the wake of a bunch, the contribution of the particles that are in Case B is given by

$$\begin{aligned} W(s) &= \int_{s-R\phi^3/24}^{s} w(s-s')\lambda(s')ds' \\ &= -\frac{2}{(3R^2)^{1/3}}\int_{s-R\phi^3/24}^{s}\lambda(s')ds'\frac{\partial}{\partial s'}\frac{1}{(s-s')^{1/3}} \\ &= \frac{4}{R\phi}\lambda\left(s - \frac{R\phi^3}{24}\right) + \frac{2}{(3R^2)^{1/3}}\int_{s-R\phi^3/24}^{s}\frac{1}{(s-s')^{1/3}}\frac{\partial\lambda(s')}{\partial s'}ds' , \end{aligned} \tag{10}$$

where we used integration by parts. Adding Eqs. (8) and (10) gives the result that agrees with Eq. (87) of Ref. [3].

2.3 Case C

Consideration in case C follows closely the case A above. We use dimensionless x ($x/R \to x$) where x is the distance from the observation point to the exit from the magnet. We also keep only the first term in Eq. (34) of Ref. [3], assume $y \gg \phi_{\rm m}\,, x$, and neglect small terms:

$$w = -\frac{4}{R^2}\gamma^2 y^3 \frac{\gamma^2\phi_{\rm m}^2(\phi_{\rm m}+2x)}{(y^2+\gamma^2\phi_{\rm m}^2(\phi_{\rm m}+2x)^2/4)^3}\,. \tag{11}$$

Introducing $\xi = y/\gamma$ we use Eq. (35) to relate ξ to $s-s'$, again keeping terms up to order of γ^{-1}

$$\frac{s-s'}{R} = \frac{1}{6}\phi_{\rm m}^2(\phi_{\rm m}+3x) + \frac{1}{2\gamma}\xi - \frac{1}{8\gamma\xi}\phi_{\rm m}^2(\phi_{\rm m}+2x)^2\,. \tag{12}$$

In the limit $\gamma \to \infty$, the wake can be approximated by the delta function,

$$w \approx A\delta\left(\frac{s-s'}{R} - \frac{1}{6}\phi_{\rm m}^2(\phi_{\rm m}+3x)\right)\,. \tag{13}$$

To find the coefficient A, we integrate w over s, using the relation $ds/R = (d\xi/2\gamma)(1+\phi_{\rm m}^2(\phi_{\rm m}+2x)^2/4\xi^2)$ that follows from Eq. (12)

$$\begin{aligned}\int w ds &= -\frac{2\phi_{\rm m}^2(\phi_{\rm m}+2x)}{R}\int_0^\infty \frac{\xi^3(1+\phi_{\rm m}^2(\phi_{\rm m}+2x)^2/4\xi^2)}{(\xi^2+\phi_{\rm m}^2(\phi_{\rm m}+2x)^2/4)^3}d\xi \\ &= -\frac{4}{R(\phi_{\rm m}+2x)}\,.\end{aligned} \tag{14}$$

This gives

$$w = -\frac{4}{R^2}\frac{1}{(\phi_{\rm m}+2x)}\delta\left(\frac{s-s'}{R} - \frac{1}{6}\phi_{\rm m}^2(\phi_{\rm m}+3x)\right)\,, \tag{15}$$

with the wake of a bunch

$$W(s) = -\frac{4}{R}\frac{1}{(\phi_{\rm m}+2x)}\lambda\left(s - \frac{R}{6}\phi_{\rm m}^2(\phi_{\rm m}+3x)\right)\,. \tag{16}$$

In the limit $x=0$, this equation reduces to Eq. (8) in which $\phi = \phi_{\rm m}$.

Note that this wake has about the same formation length $l_{\rm form}$ as in case A.

2.4 Case D

The wake in this case is given by Eqs. (36) and (37) of Ref. [3]. In the limit $\gamma \to \infty$, they take the form

$$w(s-s') = -\frac{32}{R^2}\frac{(\psi+x)^2}{\psi^2(\psi+2x)^4}\,, \tag{17}$$

where ψ is related to $s-s'$ through the equation

$$s-s' = \frac{R\psi^3}{24}\frac{\psi+4x}{\psi+x}\,. \tag{18}$$

Here again x is a dimensionless distance x/R of the observation point, measured from the exit of the magnet. The value of ψ should be smaller than ϕ_m — the maximum bending angle for the magnet, otherwise we are in the case C. This sets a limit for the maximum value $\Delta s_{\max}$ for the difference $s-s'$, which is defined by

$$\Delta s_{\max} = \frac{R\phi_m^3}{24}\frac{\phi_m+4x}{\phi_m+x}\,. \tag{19}$$

For values of $s-s' > \Delta s_{\max}$ one should use the results of case C.

Note now that the wake Eq. (17) can be cast into the following form

$$w(s-s') = -\frac{4}{R}\frac{\partial}{\partial s'}\frac{1}{\psi+2x}\,. \tag{20}$$

Indeed

$$\begin{aligned}
-\frac{\partial}{\partial s'}\frac{1}{\psi+2x} &= \left(-\frac{\partial}{\partial\psi}\frac{1}{\psi+2x}\right)\left(\frac{1}{\partial s'/\partial\psi}\right) \\
&= \frac{1}{(\psi+2x)^2}\times\frac{-8(x+\psi)^2}{\psi^2(\psi+2x)^2} \\
&= -8\frac{(\psi+x)^2}{\psi^2(\psi+2x)^4}\,.
\end{aligned} \tag{21}$$

This expression simplifies the wake for a bunch

$$\begin{aligned}
W(s) &= \int_{s-\Delta s_{\max}}^{s} w(s-s')\lambda(s')ds' \\
&= -\frac{4}{R}\int_{s-\Delta s_{\max}}^{s}\lambda(s')ds'\frac{\partial}{\partial s'}\frac{1}{\psi+2x} \\
&= \frac{4}{R}\left[\frac{\lambda(s-\Delta s_{\max})}{\phi_m+2x} + \int_{s-\Delta s_{\max}}^{s}\frac{1}{\psi+2x}\frac{\partial\lambda(s')}{\partial s'}ds'\right]\,,
\end{aligned} \tag{22}$$

where integration by parts has been used. It is easy to check that if $x = 0$ (the observation point is at the exit from the magnet) then the integral Eq. (22) reduces to Eq. (10), as expected.

3 Numerical Examples

The CSR wakefields for an arbitrary bunch distribution, $\lambda(s)$, are computed using a computer program which evaluates Eqs. (8), (10), (16), and (22) at progressive locations along a particular beamline. A simple example with a gaussian bunch passed through a single bend magnet followed by a drift length is illustrated below.

3.1 A Single Bend Magnet and Drift Section

A gaussian bunch with energy 150 MeV, charge $q = 1$ nC, and rms bunch length $\sigma_s = 50$ μm, is passed through a bend with R = 1.5-m radius. Figure 1 shows the evolution of the CSR wakefield (scaled by the bunch charge, q) from the start of the 50-cm long bend magnet through to its end, depicting cases A and B in Eqs. (8) and (10). The wakefield is plotted at 2, 5, 10, 14, 18, and 50 cm past the entrance of the magnet, which is chosen to allow immediate comparison with Fig. 2 in Ref. [4]. The CSR wakefield progresses through a transient regime at bend entrance and eventually achieves a steady-state condition (labeled "s-s" in the plot). This steady-state condition is nearly achieved at a distance from magnet entrance $L_0 = (24\sigma_s R^2)^{1/3}$ [4], which is 14 cm in this example and referred to as the "overtaking length". Note that for purposes of illustration, and to allow comparison with reference [4], the wakefields do not act back on the bunch in this simple example.

Figure 2 shows the continued evolution of the CSR wakefield beyond the bend magnet exit, through a drift section, depicting cases C and D in Eqs. (16) and (22). The plot shows the wakefield for the same 50-μm gaussian bunch at 0, 2, 5, 10, 20, and 50 cm past the exit face of the bend magnet (compare to Fig. 3 in reference [4]). The curve for $\Delta L = 0$ (blue) is the steady-state field and is identical to the curve at L = 50 cm ("s-s") in Fig. 1. In this case, the wakefield retains its shape but the amplitude drops off as the bunch propagates farther past the exit of the bend magnet.

A second bend-exit case is also depicted in Fig. 3 where the bend exit occurs well before steady-state conditions are achieved. Here the bend mag-

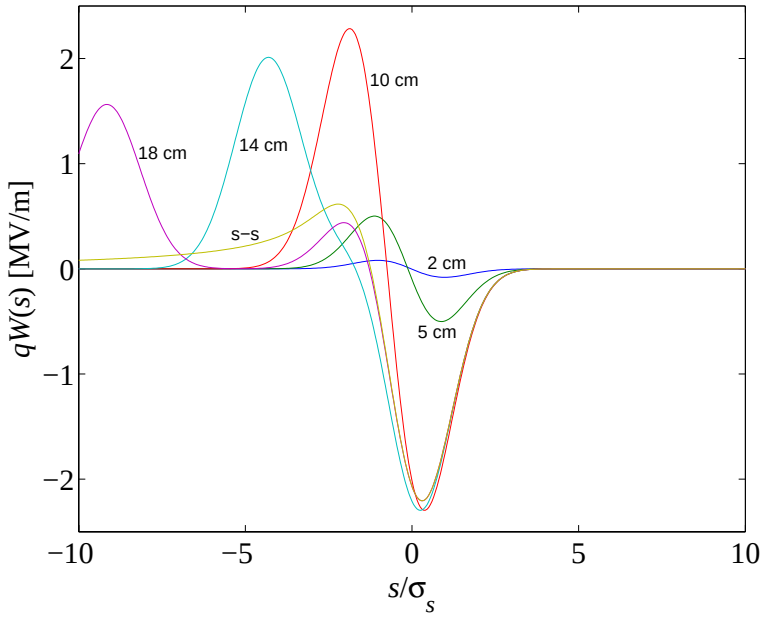

Figure 1: CSR entrance wakefield (times charge, q) at various distances past bend magnet entrance ("s-s" is steady-state). Bunch charge is $q = 1$ nC, bend radius $R = 1.5$ m, and rms bunch length $\sigma_s = 50$ μm. Bunch head is at left (compare with Fig. 2 in reference [4]). Energy loss is at negative values here.

net is set to 10-cm in length with the same $R = 1.5$-m radius and the same electron bunch. The CSR wakefield develops as in Fig. 1 until the point $L = 10$ cm (third curve in Fig. 1). At this point the bend magnet terminates and the CSR wakefield evolves as shown in Fig. 3 (no comparable figure in reference [4]). The wakefield is shown at 0, 2, 5, 10, 20, and 50 cm past the exit face of the 10-cm long bend magnet. In this transient-exit case, the CSR wakefield is not constant in shape. The amplitude, however, tapers off at a similar rate with that shown in Fig. 2.

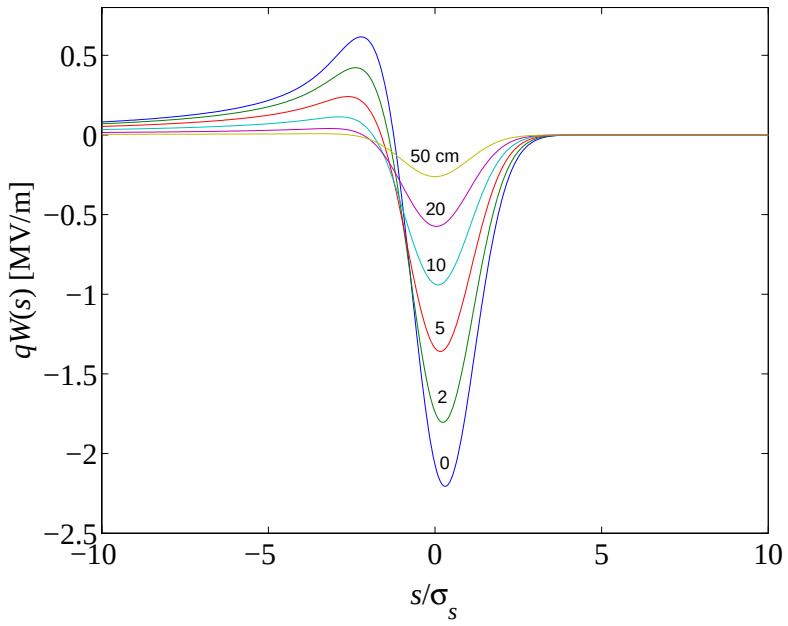

Figure 2: CSR exit wakefield at various distances (in cm) from exit of 50-cm long bend magnet with $R = 1.5$ m, $q = 1$ nC, $\sigma_s = 50$ μm (compare to Fig. 3 in reference [4]).

For the case with a 50-cm long magnet, the integrated energy loss, $\langle \Delta E \rangle$, and rms energy spread, $\langle (\Delta E - \langle \Delta E \rangle)^2 \rangle^{1/2}$, along the beamline are shown in Fig. 4, with energy loss shown as a positive value. The loss and spread for the 10-cm magnet are shown in Fig. 5. In both cases the overtaking length, L_0, is shown at 14 cm and the bend magnet exit face is shown at 50 and 10 cm, respectively.

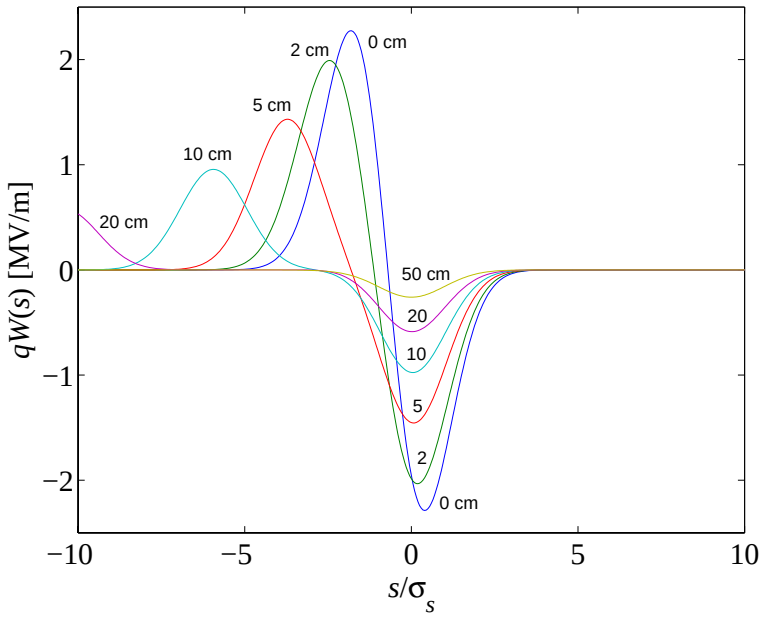

Figure 3: CSR exit wakefield at various distances (in cm) from exit of 10-cm long bend magnet with R = 1.5 m. In this case the bend-exit occurs before steady-state fields have been reached.

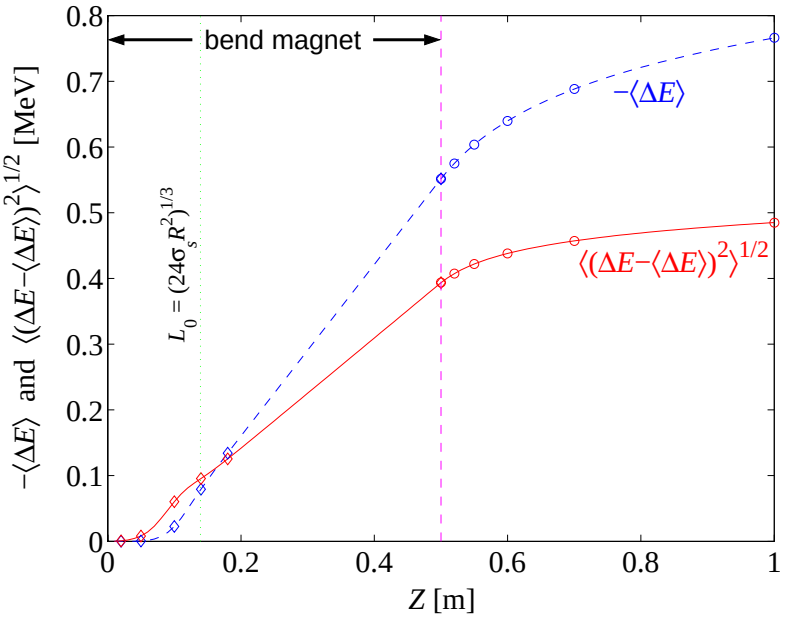

Figure 4: Energy loss (blue), $\langle\Delta E\rangle$, and rms energy spread (red), $\langle(\Delta E - \langle\Delta E\rangle)^2\rangle^{1/2}$, along 50-cm bend magnet and its exit drift section. The diamonds are the locations corresponding to the curves in Fig. 1, while the circles are the locations corresponding to the curves in Fig. 2.

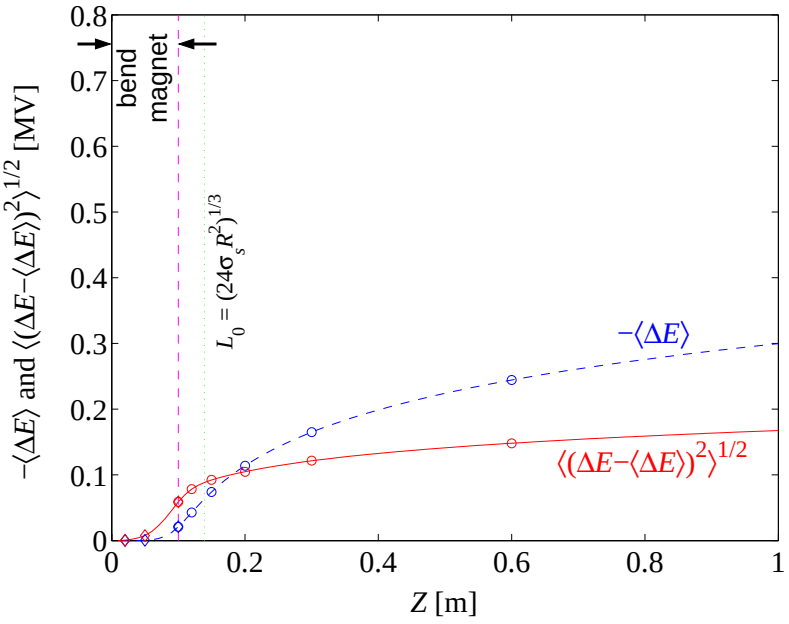

Figure 5: Energy loss (blue), $\langle\Delta E\rangle$, and rms energy spread (red), $\langle(\Delta E - \langle\Delta E\rangle)^2\rangle^{1/2}$, along 10-cm bend magnet and its exit drift section. The diamonds are the locations corresponding to the first three curves in Fig. 1, while the circles are the locations corresponding to the curves in Fig. 3.

References

[1] J. B. Murphy, S. Krinsky, and R. L. Gluckstern, in *Proc. IEEE Particle Accelerator Conference and International Conference on High-Energy Accelerators, Dallas, 1995* (IEEE, Piscataway, NJ, 1996), (IEEE Conference Record 95CH35843).

[2] Y. S. Derbenev, E. L. S. J. Rossbach, and V. D. Shiltsev, *Microbunch Radiative Tail-Head Interaction*, Tech. Rep. TESLA-FEL 95-5, Deutsches Elektronen-Synchrotron, Hamburg, Germany (Sep 1995).

[3] E. L. Saldin, E. A. Schneidmiller, and M. V. Yurkov, Nuclear Instruments and Methods, Sec. A **398**, 373 (1997).

[4] M. Dohlus and T. Limberg, Nuclear Instruments and Methods **A393**, 490 (1997).